BMC Medical Genomics

RESEARCH

Open Access

Study on the mechanism of BGN in progression and metastasis of ccRCC

Hanqing Xia[1†], Tianzhen He[2†], Xueyu Li[1], Kai Zhao[1], Zongliang Zhang[1], Guanqun Zhu[1], Han Yang[1], Xuechuan Yan[1], Qinglei Wang[1], Zhaofeng Li[1], Zaiqing Jiang[1], Ke Wang[1] and Xinbao Yin[1*]

Abstract

Purpose To investigate the role of Biglycan(BGN) in the progression and metastasis of clear cell renal cell carcinoma**(**ccRCC).

Methods Based on multiple public databases, we investigated the expression level of BGN in ccRCC, its clinical significance, and its association with immune cells. Real-time fluorescence quantitative polymerase chain reaction(PCR) was employed to validate BGN expression in tumor and adjacent normal tissues from ten patients. We utilized RNA sequencing results for further analysis, including differential gene analysis, GO-KEGG analysis, and GSEA analysis, to identify the signaling pathways through which BGN exerts its effects. BGN knockdown cells(786–0 and Caki-1) were generated through lentiviral transfection to examine the impact of BGN on ccRCC. Cell proliferation, migration, and invasion were assessed using CCK8, colony formation, wound healing, Transwell migration, and invasion assays, respectively.

Results Our findings from database analysis and PCR revealed a significant upregulation of BGN expression in kidney cancer tissues compared to normal tissues. Further analysis demonstrated a correlation between high BGN expression and ccRCC progression and immune infiltration. In vitro experiments confirmed that BGN silencing effectively inhibited cell proliferation, migration, and invasion of ccRCC. Mechanistically, these effects may be mediated through the MAPK signaling pathway.

Conclusion BGN potentially plays a pivotal role in the progression and metastasis of ccRCC, possibly acting through the MAPK signaling pathway. Therefore, BGN holds promise as a potential therapeutic target for ccRCC.

Keywords Clear cell renal cell carcinoma, Biglycan, Bioinformatics, Prognosis biomarker, Cell proliferation, Cell migration

Introduction

Clear cell renal cell carcinoma (ccRCC) is the predominant histological subtype of renal cell carcinoma (RCC), representing approximately 75% of all RCC cases, which is a prevalent urinary system malignancy characterized by a high metastasis rate and a dismal 5-year survival rate following metastasis [1, 2]. In 2022, China and the United States recorded over 70,000 new ccRCC cases, with estimated deaths of 46,345 in China and approximately 15,259 in the United States [3]. Notably, ccRCC often presents without overt clinical manifestations in its early stages, leading to most diagnoses

†Hanqing Xia and Tianzhen He these authors contributed to the work equally and should be regarded as co-first authors.

*Correspondence:
Xinbao Yin
qq127192@163.com
[1] Department of Urology, The Affiliated Hospital of Qingdao University, Qingdao, Shangdong, China
[2] Institute of Special Environmental Medicine, Nantong University, Nantong, China

being made incidentally through physical examinations [4]. Consequently, we believe that the disparity in renal cancer mortality rates between China and the United States may be attributed to the lack of early screening for renal cancer patients in China, leading to many cases being diagnosed at advanced stages [5]. Surgery remains the first-line treatment for non-metastatic ccRCC, generally yielding an excellent postoperative prognosis. However, the 5-year survival rate plummets once distant metastasis occurs [6]. Hence, elucidating the key targets of renal clear cell carcinoma and identifying a stable biomarker for early ccRCC detection and improved patient outcomes is of paramount importance. Biglycan (BGN) is a member of the Class 1 family of small leucine-rich proteoglycans (SLRP). It participates in forming the extracellular matrix and plays an essential role in building collagen fibers and cell signal transduction [7, 8]. BGN is expressed in various cells, such as bones, blood vessels, intestines, etc. Increased or decreased expression can cause multiple diseases, such as atherosclerosis [9], inflammation [7], skeletal development disorders [10], atherosclerosis [11], and malignant tumors [8]. Its expression is elevated in a variety of tumors, and patients with elevated expression are associated with poorer prognosis, so it may have the potential to become a prognostic marker. Its molecular mechanism has yet to be fully elucidated. Still, it is currently considered to be related to the nuclear factor-kappa B (NF-κB) and extracellular signal-regulated kinase (ERK) signaling pathways [12]. Many articles view it as a marker that reflects prognosis and is closely related to immunotherapy in colon cancer [13–15]. Among them, Liu Bin et al. explored that biglycan promotes the NF-κB signaling pathway, reducing the sensitivity of colon cancer chemotherapy [16].

This study employed TCGA, GTEX, HPA, and UALCAN datasets, along with the Kaplan–Meier (KM) plotter web tool, to analyze BGN expression, its association with other genes, and its clinical significance. Concurrently, RNA sequencing was utilized to unravel the potential biological functions of BGN in ccRCC, leading to the hypothesis that it may function through the MAPK signaling pathway. Subsequently, the influence of BGN expression on immune infiltration was verified. Finally, in vitro experiments using ccRCC cells were conducted to assess the impact of BGN on ccRCC progression.

To summarize, our investigation elucidated the elevated expression of BGN across various tumors and its implications for patient prognosis. We specifically delved into its expression in ccRCC, the impact of its increased expression on patients, its effect on cells in vitro, and its potential mechanism of action. Based on these findings, we posit BGN as a promising prognostic marker for ccRCC.

Materials and methods

Data source

A ccRCC dataset comprising genome data and associated clinical information for 539 tumor and 72 normal samples was obtained from the TCGA database (https://portal.gdc.cancer.gov/repository). Similarly, ccRCC microarray data of GSE65615 from the Gene Expression Omnibus (GEO) database (http://www.ncbi.nlm.nih.gov/geo/) includes clinical genomic data and associated clinical data for 122 tumors and 16 normal samples.

Procurement of pathological tissue

This study included clinical data from ten patients diagnosed with ccRCC who underwent laparoscopic radical or partial nephrectomy at the Affiliated Hospital of Qingdao University in May 2022. All participants were undergoing their first renal surgery, had no other primary tumors, and had not received any preoperative treatments to inhibit tumor growth. Pathological examination confirmed that the intraoperative collected cancer tissue specimens were indeed renal clear cell carcinoma, with cancerous tissue comprising over 90%, while adjacent tissue was identified as renal tissue. The adjacent tissue specimen was collected from a region at least 1 cm distant from the tumor margin. Informed consent regarding the collection and application of tissue specimens was thoroughly explained to the patients, who signed the consent form after careful consideration. This research was conducted in accordance with ethical guidelines from the Declaration of Helsinki, following approval from the Medical Ethics Committee of the Affiliated Hospital of Qingdao University (Ethics No.: QYFYWZLL26556). During the procedure, renal clear cell carcinoma tissue and adjacent renal tissue were fixed in formalin, placed in cryovials, rapidly frozen in liquid nitrogen, and stored at −80 °C for subsequent PCR experiments.

Real-time RT-PCR assay

In the real-time RT-PCR assay, we extracted RNA from tissues in accordance with PCR experimental requirements. and then used an RT kit (servicebio, Wuhan) for reverse transcription. The primers used in this study are as follows:H-GAPDH-S: GGAAGCTTGTCATCAATG. GAAATC, H-GAPDH-A: TGATGACCCTTTTGGCTC CC; H-BGN-S:GACCTGGGTCT GAAGTCTGTGC,H-BGN-A: GTTGTTCACCAGGACGAGGG.

The human protein atlas

This study utilized the HPA (Human Protein Atlas) database to examine the protein expression of BGN in

ccRCC tissues [17]. The HPA, based on proteomics, transcriptomics, and systems biology data, generates spatial expression maps of proteins across various tissues, cells, and organs.

Cell culture

The ccRCC cell lines 786–0 and Caki-1 were obtained from Wuhan Punosai Biotechnology Co., China and maintained in DMEM (PM150210, Procell Life Science & Technology) supplemented with 10% fetal bovine serum (FBS) (164,210–50, Procell Life Science & Technology) and incubated at 37 °C in a 5% CO_2 incubator.

Establishment of stable cell lines via lentiviral transduction

The lentivirus and reagents required for transfection (purinomycin and polybrene reagent) were provided by Heyuan Biotechnology Co., LTD (Shanghai, China). The cells were digested and prepared into a suspension with a concentration of 4×10 [3] cells/mL. After adding 500 μL of this suspension to each well of a 24-well plate, the wells ware incubated overnight. Next, 2.5 μL of a 5 mg/mL polybrane reagent was added to each well, followed by the addition of lentivirus. After 16 h of transfection, the medium was replaced, and the cells were continued in culture. The fluorescence of the cells was monitored regularly, and, after the addition of puramycin to the cells, reaching a final concentration of 2 μg/mL, cells can underwent subsequent experiments following three generations of selection.

Western blot analysis and antibodies

In brief, cells were washed and lysed with RIPA (E-BC-R327, Elabscience Biotechnology Co.) lysis buffer to extract the protein solution. The concentration of extracted proteins was determined using the Bicinchoninic Acid (BCA) method. Extracted proteins were boiled at 100 °C for 15 min and separated using sodium dodecyl sulfate–polyacrylamide gel electrophoresis (SDS-PAGE). The protein was then transferred to a 0.45 μm polyvinylidene fluoride membrane blocked with skim milk and incubated with the corresponding primary and secondary antibodies. Finally, ECL detection reagents were used to visualize the protein signal and analyze data. The primary antibodies were BGN (Abcam, 1:2000 dilution) and GADPH (Elabscience Biotechnology Co., 1:5000 dilution).

Cell counting kit-8 (CCK-8) assay

Caki-1 and 786–0 cells with transfection were plated into 96-well plates(1000 cells/well). 10 μL of CCK-8 reagent (HY-K0301, MCE, USA) were added to each well at specified time points(24, 48, 72, 96 and 120 h). The plates, wrapped in aluminum foil, were placed in the incubator for 1 h. Subsequently, the absorbance at 450 nm was measured using a microplate reader..

Cell proliferation and cell migration assay

For the transwell migration assay, 600 μL of medium containing 10% FBS was added to the lower layer of the culture chamber. Next, 100 μL of single-cell suspension containing 2×10^4 cells was added to the upper chamber, and the cells were cultured for 12 h. After incubating the cells for 24 h, they were fixed, washed, and stained with 0.5% crystal violet. Images were then obtained under a microscope.

RNAseq analysis

Cells were lysed in TRIzol (9108, Takara, Japan). RNA samples extracted from the cells were sent to genedenovo Biotechnology Co., Ltd.(Guangdong, China) for follow-up experiments: Total RNA was extracted from the samples using appropriate kits to remove rRNA and enrich mRNA. Subsequently, the enriched mRNA was reverse-transcribed to generate double-stranded cDNA. Following cDNA end repair, adapters were ligated, and PCR amplification was performed. A computer-controlled library was constructed, and library quality was assessed. Finally, a series of analyses were conducted, including GO-KEGG analysis, DO research, GSEA analysis, and others.

Colony formation assay

Caki-1 and 786–0 cells with transfection were plated into 6-well plates (150 cells per well) and maintained for two weeks to induce colony growth. The colonies were then fixed with 4% paraformaldehyde and stained with 0.1% crystal violet. Each group was replicated in three wells.

Statistical analysis

Data analysis was performed using R software version v3.6.3. The "ggplot2", "survminer", and "survival" R packages were used to generate expression analysis and KM survival curves. Log-rank tests were employed to assess statistical significance. Univariate Cox proportional hazards regression was used to estimate *p*-values and hazard ratios (HRs) with 95% confidence intervals (CIs) in KM curves. Two-gene correlation analysis was performed using the R package "ggstatsplot". Correlations between quantitative variables were evaluated using Pearson's or Spearman's correlation analysis. Data from the BGN functional assay were statistically analyzed using GraphPad Prism 7.0. Statistical significance was determined based on *p*-values: $^{*}p<0.05$, $^{**}p<0.01$, $^{***}p<0.001$, $^{****}p<0.0001$.

Results

BGN expression levels in pan-cancer and normal tissues

We analyzed the expression levels of BGN in tumor tissues and corresponding normal tissues of pan-cancer patients using data from the TCGA and GTEx databases. Our findings indicate that BGN expression is up-regulated in 15 types of tumors compared to normal tissues (Fig. 1A). Additionally, we examined expression data of BGN in paired cancer tissues and adjacent normal tissue samples from human cancers, also obtained from the TCGA database and GTEx databases. This analysis revealed that 15 types of tumor tissues exhibit elevated BGN expression compared to their normal counterparts (Fig. 1B). To investigate the potential prognostic value of BGN, we collected BGN mRNA expression levels and patient overall survival (OS) data for pan-cancer and adjacent normal tissue types in the TCGA database. We then performed KM survival analysis and log-rank tests to assess the relationship between BGN expression and patient survival. Our results demonstrate that higher BGN expression levels are significantly associated with poor prognosis in four types of cancer: ccRCC (clear cell renal cell carcinoma), KIRP (kidney renal papillary cell carcinoma), STAD (stomach adenocarcinoma), and HNSC (head and neck squamous cell carcinoma) (Fig. 1C). These findings underscore the significance of BGN expression and its prognostic implications in pan-cancer.

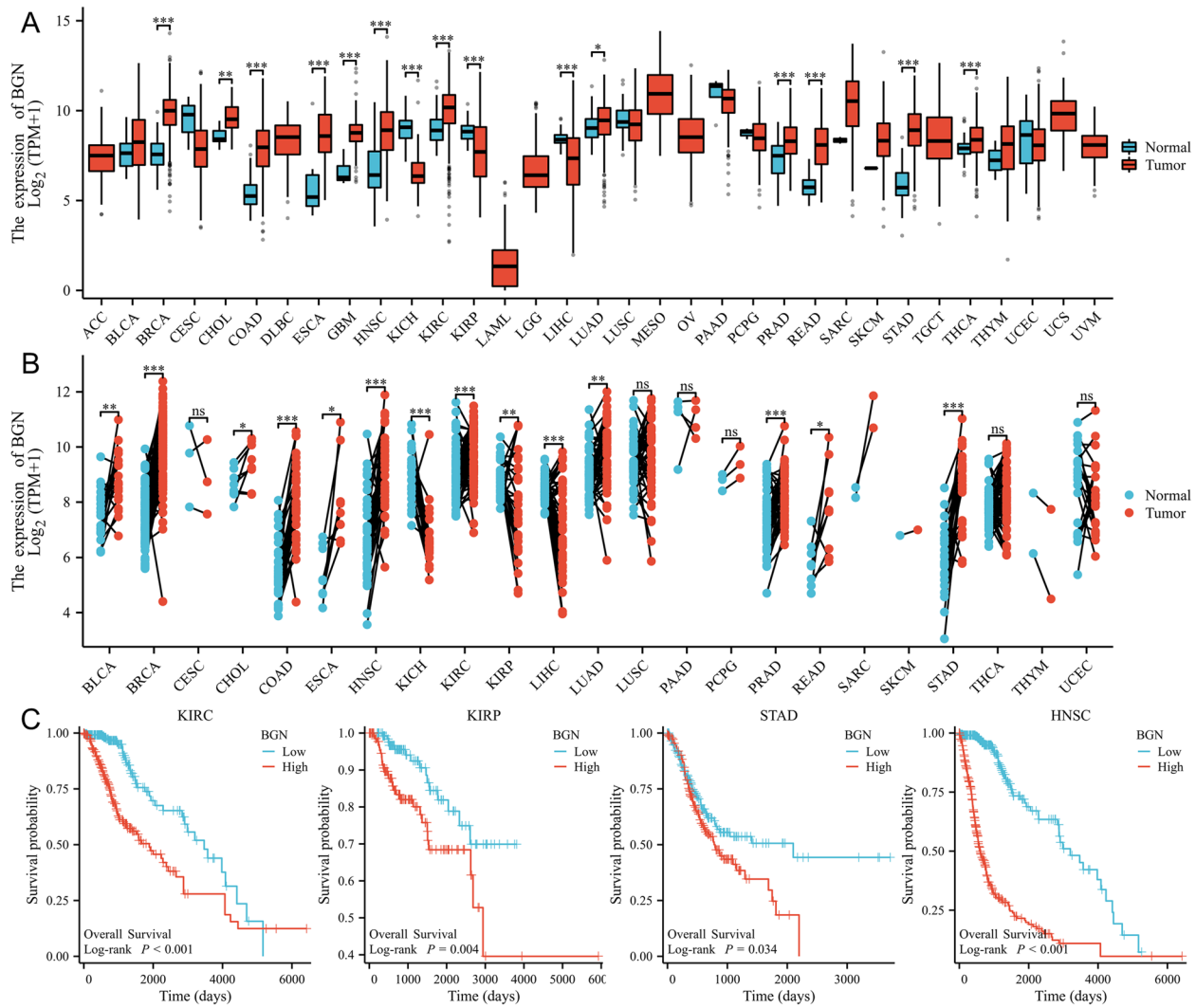

Fig. 1 Expression pattern and prognostic value of BGN from the perspective of pan-cancer. **A** BGN expression levels in different tumor tissues and adjacent normal tissues from TCGA and GTEx databases. **B** BGN expression levels in paired cancer tissues and adjacent normal tissue samples from human cancer (**C**) Prognostic analysis of BGN mRNA expression levels in various human cancers. NS, $p > 0.05$, $^{*}p < 0.05$, $^{**}p < 0.01$, $^{***}p < 0.001$

BGN expression is increased in ccRCC

We conducted a comprehensive evaluation of BGN expression levels in ccRCC, and the results consistently demonstrated elevated BGN expression in tumor tissues, regardless of whether paired or unpaired data was analyzed (Fig. 2A, B). To further corroborate these findings, we examined BGN expression in ccRCC using the "GSE65615" dataset from the GEO database. The results obtained align with previous studies, confirming the up-regulation of BGN in ccRCC (Fig. 2C).In addition, we performed qPCR analysis on tumor tissues and adjacent tissues from 10 ccRCC patients, further validating the increased mRNA level of BGN in ccRCC (Fig. 2D). Immunohistochemistry (IHC) staining data from the HPA database also supports the notion of BGN protein up-regulation in clear cell renal cell carcinoma (Fig. 2E). Taken together, these findings from multiple database analyses and PCR experiments consistently demonstrate the up-regulation of BGN in ccRCC, suggesting its potential role in influencing patient prognosis.

BGN overexpression was associated with poor patient prognosis

We investigated the association between BGN expression and various clinical characteristics, including TNM stage, gender, age, and histological stage. Elevated BGN expression was found to be significantly correlated with these factors (Fig. 3A-F). Additionally, logistic regression analysis revealed a significant association between BGN expression and poor clinicopathological prognosis, encompassing T stage (T3 vs. T1&T2), M stage (M1 vs. M0), gender (male vs. female), histopathological stage (G3&G4 vs. G1&G2), pathological stage (stage III&IV vs. stage I&II), race (white vs. yellow & black), and hemoglobin concentration (normal vs. increased vs. decreased) (Table 1). Collectively, these findings suggest that elevated BGN expression may be linked to adverse clinical outcomes.

Gene functional annotation and pathway analysis

We investigated the underlying mechanisms by which BGN promotes ccRCC progression and metastasis. RNA extracted from Caki-1 knockout and control cells was processed for library construction, rigorously quality checked, and subsequently sequenced. Based on the differential expression analysis, we screened for significantly different genes according to $p < 0.05$ and $|\log2FC| > \log2(1.5)$. Volcano plot analysis was performed based on the significantly different genes identified in each comparison group (Fig. 4A). The differential gene expression patterns were analyzed and the processed results were presented as heat maps (Fig. 4B). Functional annotation indicated that these genes are involved in blood vessel development,

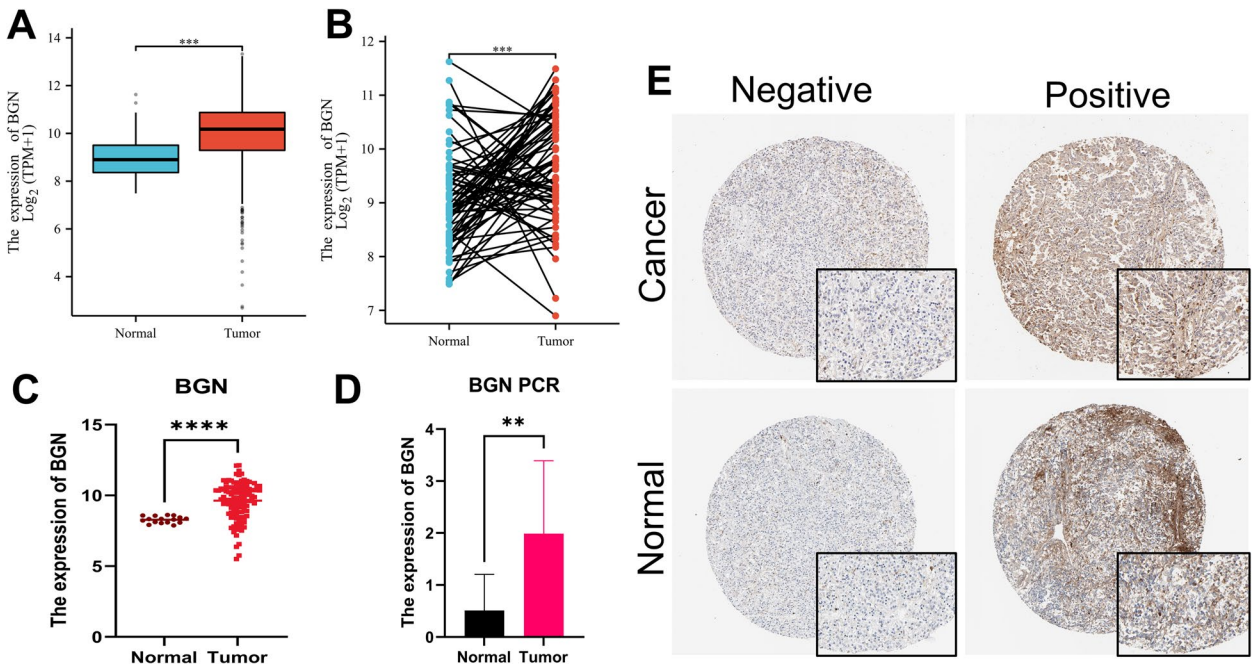

Fig. 2 Expression of BGN RNA and protein in ccRcc. **A**–**B** BGN expression levels in ccRcc tissues and normal tissues from TCGA and GTEx databases. **C** BGN expression levels in ccRcc tissues and normal tissues determined from GEO datasets. **D** BGN mRNA expression levels in ccRcc patients and matched adjacent normal samples. **E** BGN protein expression levels based on human protein atlas. $^{**}p < 0.01$ $^{***}p < 0.001$,$^{****}p < 0.0001$

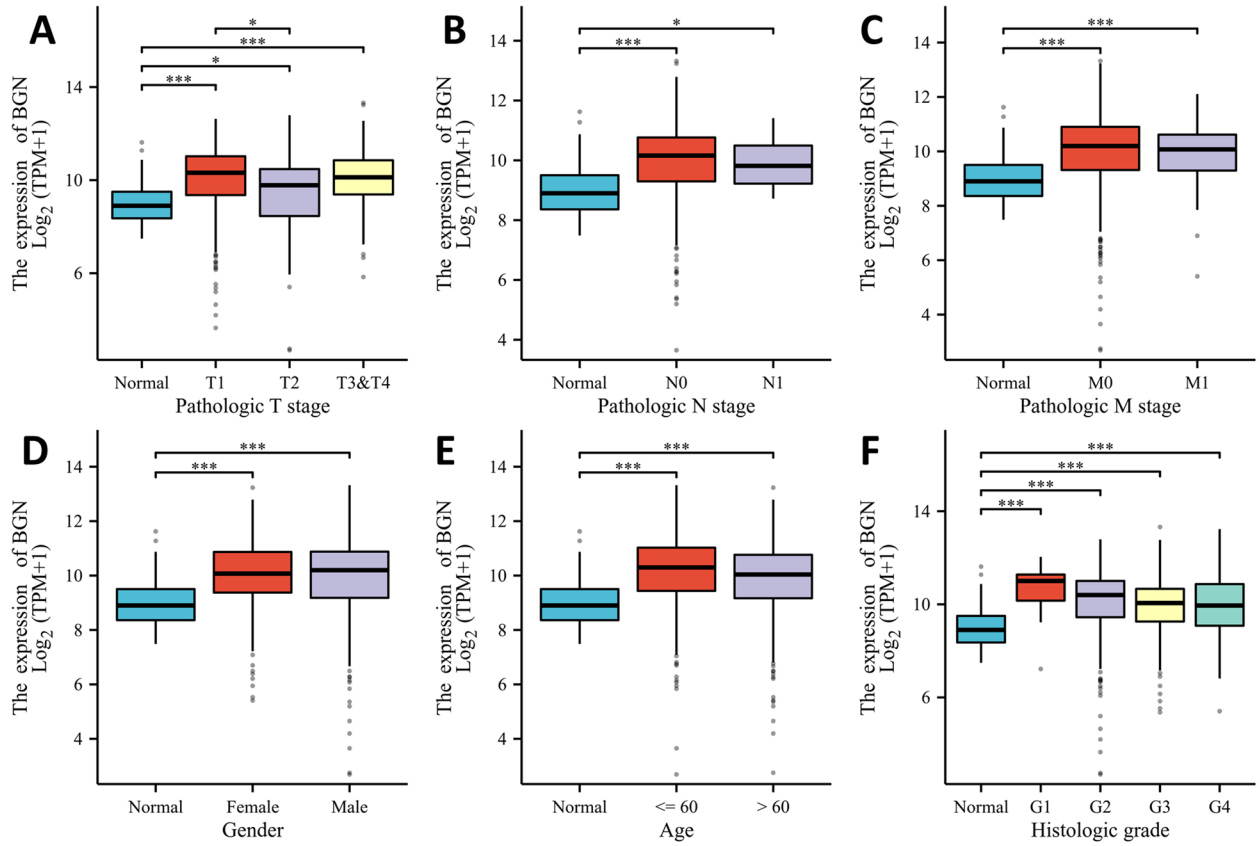

Fig. 3 Clinical significance of BGN in ccRcc. Correlation between BGN expression and clinical parameters, including (**A**-**C**) TNM stage, **D** gender, **E** age, **F** histological grade, NS, $p > 0.05$, $^{*}p < 0.05$, $^{**}p < 0.01$, $^{***}p < 0.001$

Table 1 Logistic regression analysis of the correlation between BGN expression and clinical pathological characteristics

Characteristics	Total (N)	OR (95% CI)	*P* value
Pathologic T stage (T3 vs. T1&T2)	530	0.434 (0.300—0.628)	**< 0.001**
Pathologic N stage (N1 vs. N0)	258	0.580 (0.205—1.647)	0.307
Pathologic M stage (M1 vs. M0)	508	0.411 (0.245—0.688)	**< 0.001**
Gender (Male vs. Female)	541	0.604 (0.422—0.864)	**0.006**
Age (> 60 vs. < = 60)	541	0.856 (0.611—1.200)	0.367
Histologic grade (G4&G3 vs. G1&G2)	533	0.449 (0.317—0.635)	**< 0.001**
Pathologic stage (Stage III&Stage IV vs. Stage I&Stage II)	538	0.389 (0.272—0.557)	**< 0.001**
Race (White vs. Asian&Black or African American)	534	0.368 (0.209—0.647)	**< 0.001**
Serum calcium (Normal&Elevated vs. Low)	367	0.904 (0.598—1.366)	0.631
Hemoglobin (Normal&Elevated vs. Low)	461	1.464 (1.010—2.122)	**0.044**
Laterality (Right vs. Left)	540	1.143 (0.815—1.603)	0.438

blood vessel morphogenesis, urogenital system development, cell population proliferation and others (Fig. 4C). Alterations in the biological processes (BP) and molecular functions (MF) of BGN were associated with the cell periphery, plasma membrane, plasma membrane region, extracellular region, extracellular space, molecular function regulator, signaling receptor binding, lipid binding, signaling receptor regulator activity, signaling receptor activator activity, and receptor-ligand activity (Fig. 4D-E). KEGG molecular pathways included Basal cell carcinoma, MAPK signaling pathway, Pathways in cancer, Axon guidance and

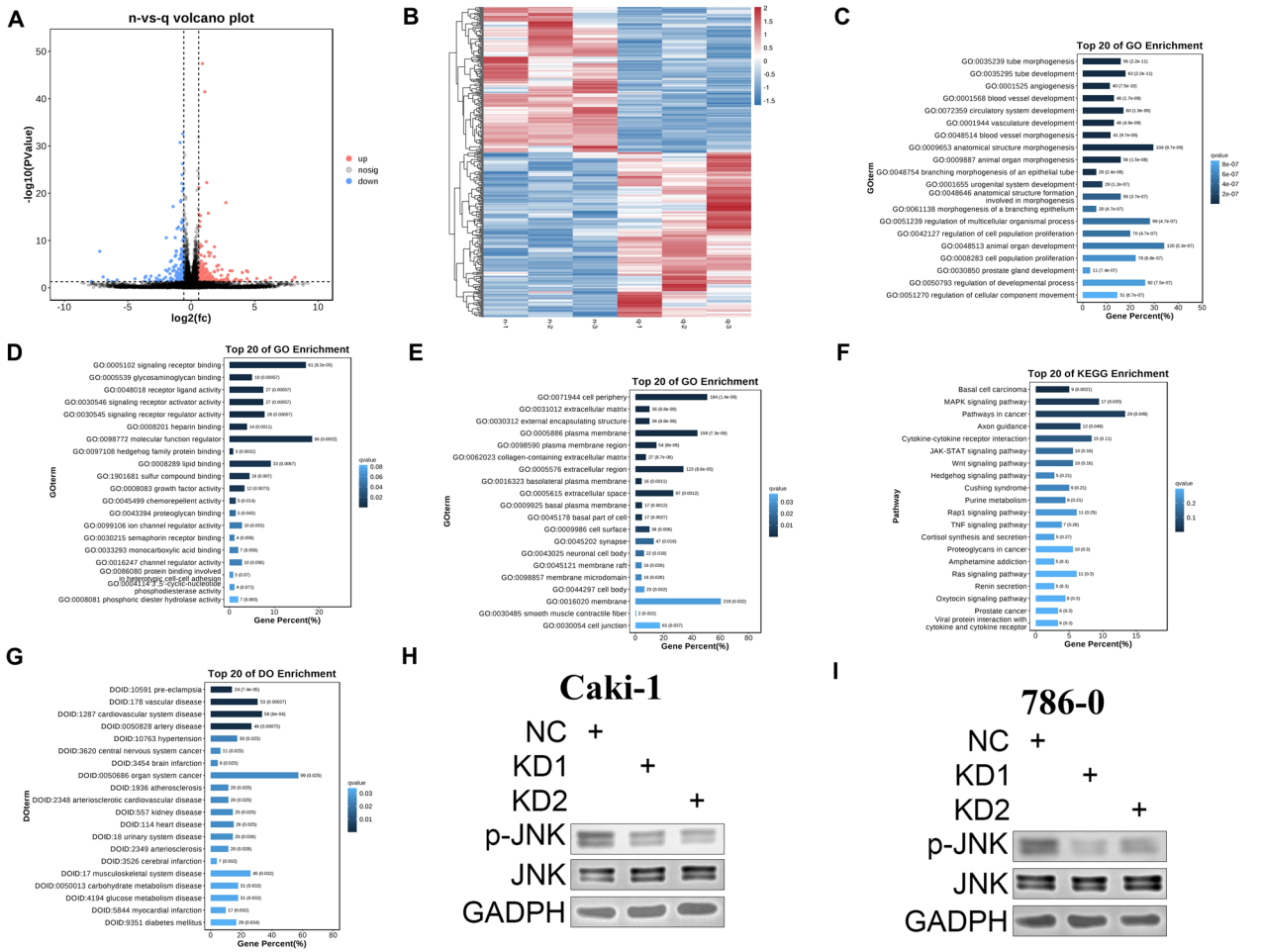

Fig. 4 Functional enrichment analysis of BGN in ccRcc. **A**–**B** The correlation analysis of BGN expression and its top 100 co-expressed gene network. **C**–**G** GO and KEGG enrichment analysis of co-expressed genes. **H**-**I** The phosphorylation of JNK decreased after BGN knockdown

others (Fig. 4F). We mapped the differential genes to each term of the DO database (http://disease-ontology.org/). We calculated the number of differential genes for each term, obtaining a list of differential genes with a particular DO function and statistics on the number of differential genes. A hypergeometric test was then applied to identify DO entries that were significantly enriched in differential genes compared to the entire background. Our research revealed that BGN expression is associated with organ system cancer, kidney disease, urinary system disease and other diseases, which further indicated that BGN had a certain relationship with the occurrence and development of renal cancer (Fig. 4G). The phosphorylation status of the MAPK signaling pathway was assessed in CAKI-1 and 786–0 cells following BGN knockdown. Our results indicated a reduction in the phosphorylation of the JNK-MAPK signaling pathway after BGN knockdown (Fig. 4H-I).

BGN-related signaling pathways based on gene set enrichment analysis

To elucidate the biological role of BGN, we analyzed the differentially expressed genes (DEGs) between the low and high BGN expression groups based on the median expression value of BGN. Gene set enrichment analysis (GSEA) pathway analysis revealed that BGN is involved in pathways closely related to cell division and immune response, which are significant to the formation of ccRCC. (Fig. 5A-F).

The relationship between BGN and immune cells and checkpoints in ccRCC

Immune cells infiltrating the tumor microenvironment have a profound impact on tumor progression and patient outcomes. Accordingly, we investigated whether elevated BGN expression influences the abundance of immune cells in the ccRCC tumor microenvironment

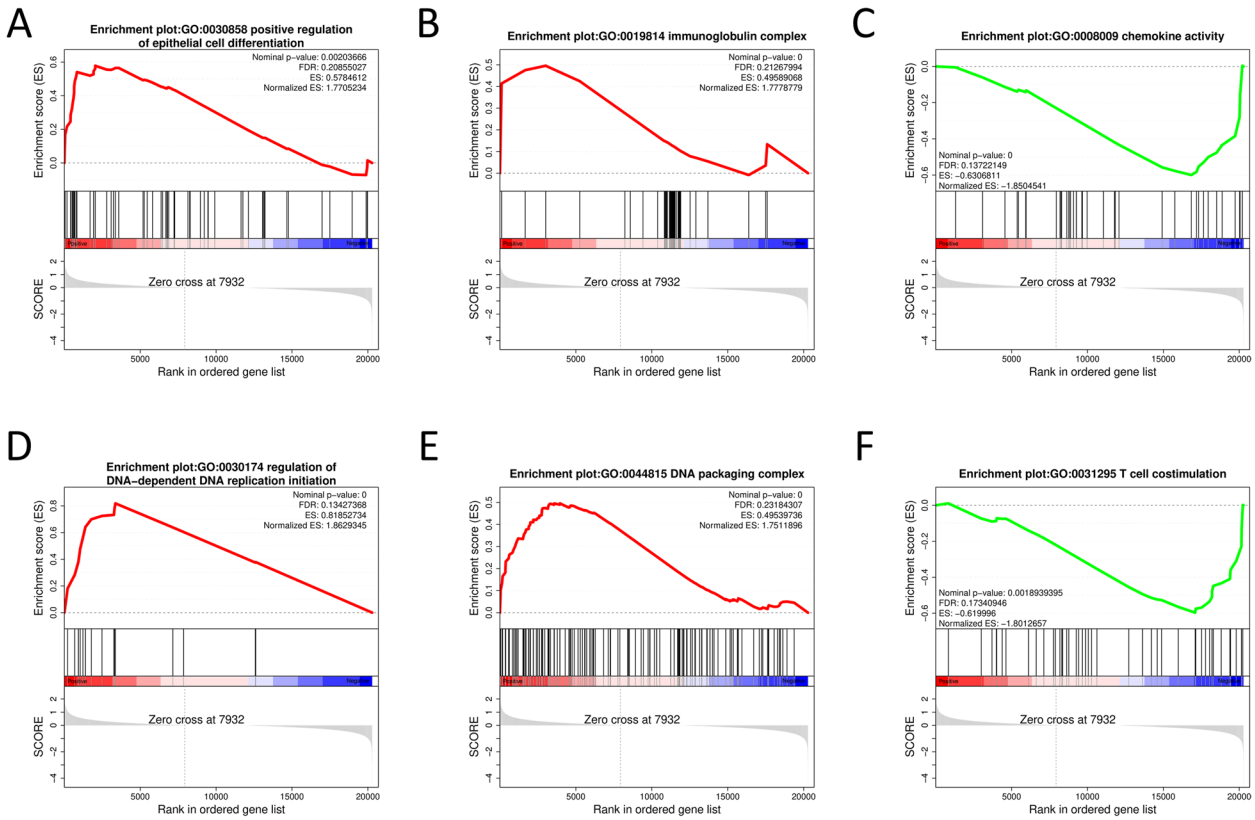

Fig. 5 **A**-**F** Identification of BGN-related signaling pathways in ccRcc. BGN is primarily involved in positive regulation of epithelial cell differentiation, immunoglobulin complex, chemokine activity, regulation of DNA-dependent DNA replication initiation, DNA packaging complex, T cell costimulation and others

and, consequently, patient prognosis. Our findings revealed that the mRNA expression level of BGN exhibits a significant positive correlation with NK cells, pDC, Tem, Mast cells, and other immune cell populations (Fig. 6A). Conversely, a negative correlation was observed with NK CD56bright cells (Fig. 6A). Given that BGN may function as a tumor-promoting gene in ccRCC, we assessed the relationship between BGN and FAM241B, TMEM37, UGT2B7, LRG1, SHCBP1, SOSTDC1, NPTX1, FAM98B, ZNF439, and ZNF440 in ccRCC (Fig. 6B). Notably, BGN expression was found to be significantly positively correlated with these genes, suggesting that BGN may be involved in immune evasion mechanisms. Subsequently, we conducted KM survival curve analysis of BGN expression at different levels of immune cell infiltration in ccRCC. Interestingly, we observed that higher BGN levels in KIRCs with reduced B-cells, CD8 + T-cells, Mesenchymal stem cells, or enriched CD4 + memory T-cells were associated with a poorer prognosis (Fig. 6C-F). In conclusion, our study demonstrates that BGN may participate in immune infiltration mechanisms and influence patient prognosis by modulating the infiltration of immune cells.

Influence of BGN on ccRCC cells in vitro experiments

This study employed lentivirus to suppress BGN expression in Caki-1 and 786–0 cells. We transfected the three knockdown virus strains provided by the vendor, conducted western blot verification to assess their effectiveness, and selected the two strains exhibiting the most significant knockdown effect for subsequent experiments (Fig. 7A-D). The cell counting kit-8 (CCK-8) assay (Fig. 7E-F), colony formation assay (Fig. 7G-H), wound healing assay (Fig. 7I-L), and transwell assays (Fig. 7M-P) collectively demonstrated that BGN depletion dramatically inhibited the proliferation, migration, and invasion capacities of ccRCC cells. These findings were statistically significant.

Discussion

The function of BGN in tumors has been extensively explored in the literature. For instance, the CS/DS chain with non-reducing end 3-O-sulfated GlcA on BGN

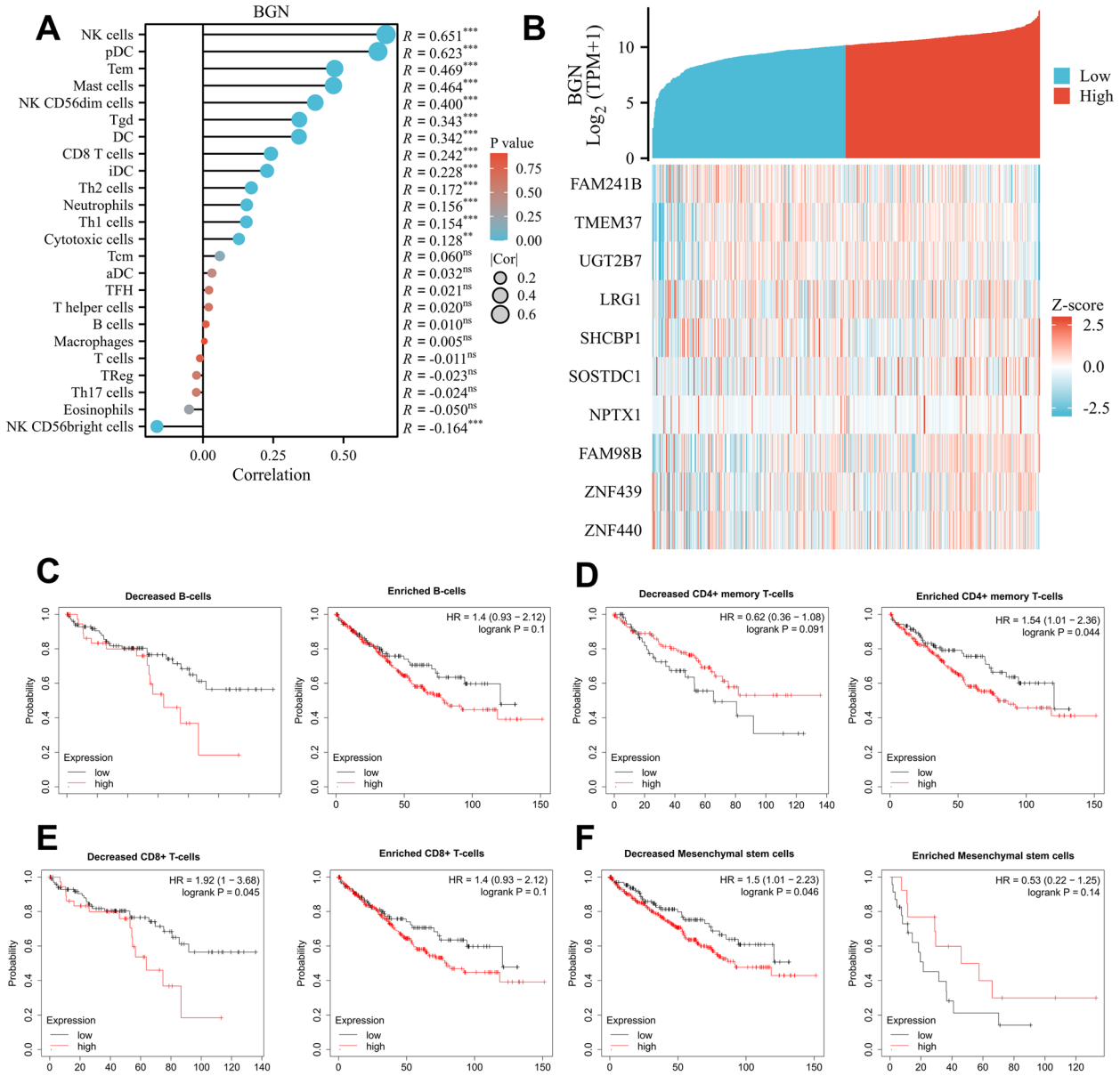

Fig. 6 Correlation analysis of BGN expression and infiltration levels of immune cells in ccRcc. **A** The correlation between BGN expression and infiltration levels of immune cells. **B** Correlation analysis of BGN expression and immune checkpoint-related genes in ccRcc in the TCGA database. **C**-**F** Correlations between BGN expression and overall survival in different immune cell subgroups in ccRcc patients were determined by the Kaplan–Meier plotter

harbors a rare bi-sulfated motif that may be implicated in cancer-associated signaling [18]; BGN has been shown to promote the development and progression of lung cancer through ECM-receptor interactions [19]; LINC00460 has been demonstrated to facilitate head and neck squamous cell carcinoma progression by upregulating BGN expression [20]. Currently, a substantial body of research delves into the mechanism of BGN in gastric cancer. For example, BGN enhances gastric cancer progression and metastasis by promoting FAK signaling pathway transduction [21]. The secretion of BGN by gastric cancer cells can induce the generation of CAF-like cells. On the one hand, these cells activate TLR signal transduction; conversely, they secrete fibroblast activation protein, further fostering gastric cancer invasion and metastasis. BGN triggers the RIP1/RIP3/MLKL signaling pathway and attenuates the release of pro-inflammatory cytokines to promote gastric cancer progression [22]. In this study,

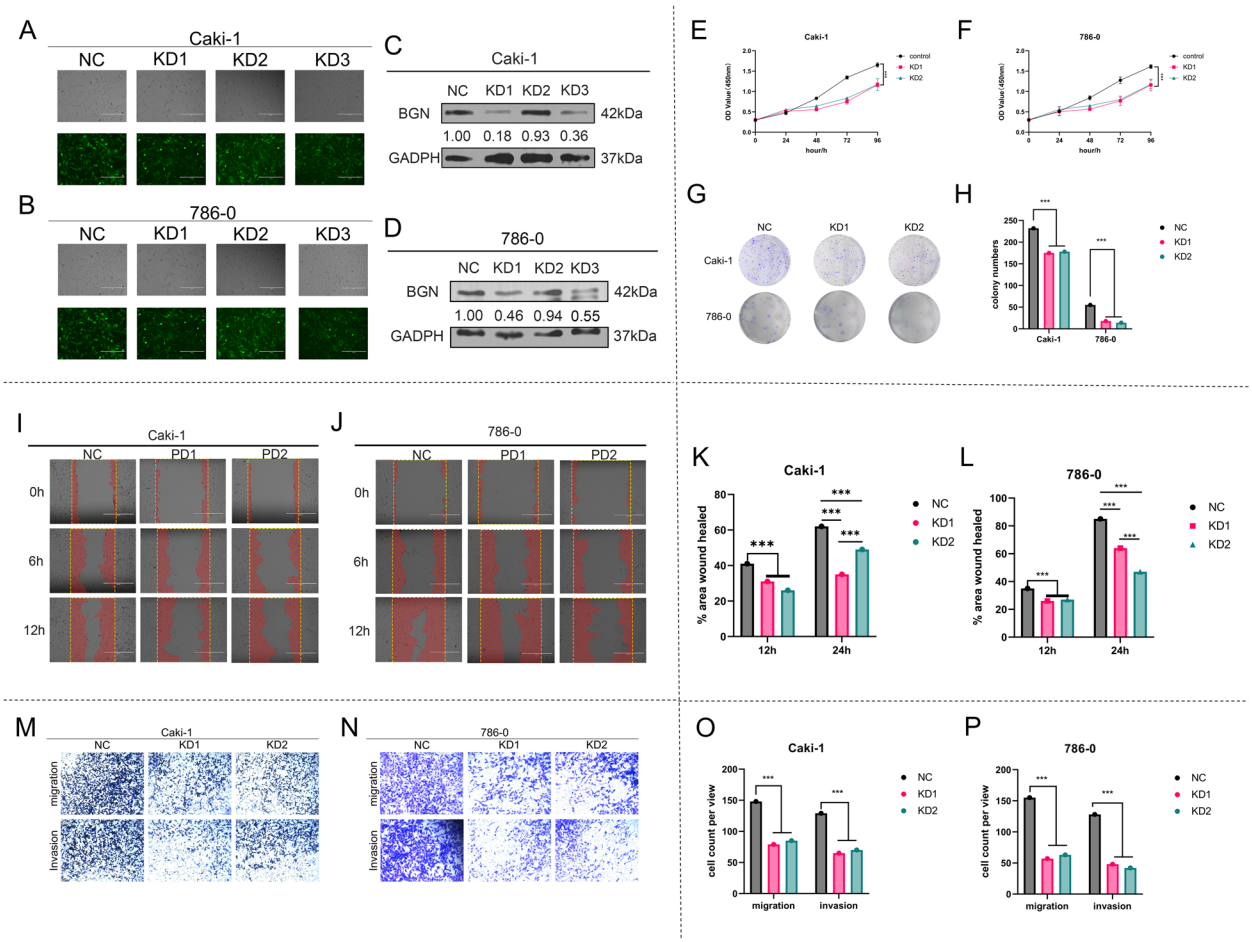

Fig. 7 Upregulation of BGN is associated with poor prognosis in ccRCC. **A**-**D** Microscopic images of renal clear cell carcinoma (caki-1, 786–0) after lentivirus transfection and BGN protein expression of cells in each group. (E–F)CCK-8 assay. **G**-**H** Colony formation assay. **I**-**L** wound healing assay. **M**-**P** Transwell assay. Data presents as mean ± SD with three replicates. ***, $P < 0.001$

BGN was found to be upregulated in some cancers using data from TCGA and GTEX databases. This finding suggests that BGN may be involved in tumor development, consistent with previous studies [23]. Subsequently, we integrated data from the database and patient pathological information, revealing that BGN expression is significantly upregulated in ccRCC. Furthermore, elevated BGN expression was correlated with a poorer prognosis in these patients.Through RNA sequencing analysis, we identified that BGN is implicated in multiple pathways associated with tumor progression, including vascular growth and immune microenvironment regulation, as well as its potential role in the pathogenesis of urinary system diseases. Notably, our findings suggest that BGN may exert its effects via the JNK-MAPK signaling pathway, that plays a crucial role in transducing extracellular signals into diverse cellular responses. Among its major components, the c-Jun N-terminal kinase (JNK) pathway is particularly significant as it regulates vital processes such as cell proliferation, differentiation, and survival [24]. Numerous studies have highlighted the significant involvement of the JNK-MAPK signaling pathway in the initiation and progression of various cancers, such as gastric, colorectal, lung cancers, and melanoma [25–28]. Building on this knowledge, our research seeks to explore the preliminary roles of this pathway in the progression of ccRCC, thereby establishing a foundation for future investigations into its specific mechanisms. In recent years, numerous studies have demonstrated a tight link between the development of certain cancers and inflammation [29, 30]. Some of the tumor-promoting effects of BGN are also associated with immune responses and inflammatory processes. For instance, soluble BGN produced by the ECM fosters inflammatory responses through Toll-like receptors (TLRs) 2/TLR4 in macrophages and dendritic cells [31]. BGN activates the nuclear translocation of NF-κB in B cells, leading to the emergence of its transcriptional effects and the activation

of p38 and ERK signaling cascades, thereby enhancing the expression of proinflammatory cytokines to trigger and regulate inflammation [32]. The expression of BGN is inversely correlated with CD8 + T cells in triple-negative breast cancer, suggesting that BGN may be involved in adaptive immune responses [33]. BGN, via the TLR4/NF-κB pathway, contributes to the epigenetic silencing of Siglec-7 ligand, an immunosuppressive molecule [34]. Research has shown that ccRCC is closely associated with the tumor immune microenvironment, and BGN is also linked to chronic renal inflammation [7, 35]. Based on the above studies, we suggested that BGN may affect the prognosis of renal cell carcinoma patients through immune infiltration. So this study investigated the relationship between BGN, immune cells, and immune checkpoints and found that the mRNA expression level of BGN was significantly positively correlated with NK cells, pDC, Tem, mast cells, and other cells. Conversely, it was negatively correlated with NK CD56bright cells. Additionally, immune cell infiltration affects patient prognosis. These findings indicate that BGN may be involved in immune evasion and anti-tumor immunity to promote ccRCC formation and influence patient prognosis. We conducted in vitro experiments to investigate the biological functions of BGN in ccRCC. The results revealed that knockdown of the BGN gene in Caki-1 and 786–0 cells significantly inhibited cell proliferation, migration, and invasion.

This study delved into the relationship and potential mechanisms between BGN and the formation and development of clear cell renal cell carcinoma (ccRCC). However, it is important to acknowledge certain limitations of the study. Firstly, the analysis suggested that BGN may influence the occurrence, growth, and apoptosis of ccRCC through immune mechanisms. However, this hypothesis was not experimentally validated, and its veracity requires further investigation. Additionally, the study was confined to in vitro experiments, and in vivo experiments were not conducted. This limits the generalizability of the findings. Furthermore, experiments to verify the role of BGN in the signal pathway were not performed, leaving this aspect unexplored.

Conclusion

This study investigated the expression level of BGN in various cancers and subsequently delved into the clinical relevance, immuno-oncology features, and biological functions of BGN in ccRCC. Notably, we postulate that BGN may exert its effects through the MAPK signaling pathway. In essence, BGN has the potential to serve as a prognostic marker for ccRCC, and further research holds the promise of advancing immunotherapy research in ccRCC.

Supplementary Information

The online version contains supplementary material available at https://doi.org/10.1186/s12920-025-02124-5.

Supplementary Material 1.

Supplementary Material 2.

Acknowledgements
Not Applicable.

Authors' contributions
KW, XBY, HQX conceived and supervised the study. TZH, HQX and XBY acquired the data. GQZ and TZH retrieved and reviewed the literature. XBY, XYL analyzed the results, and HQX, QLW, ZFL critically revised the manuscript for intellectual content. HY, XCY, HQX drafted the manuscript. KZ, TZH, XYL and ZQJ prepared figures and tables. All authors have readed and approved the final manuscript.

Funding
This research was funded by the National Science Foundation of China, Grant numbers 82200759. The funding bodies played no role in the design of the study and collection, analysis, and interpretation of data and in writing the manuscript.

Data availability
No datasets were generated or analysed during the current study.

Declarations

Ethics approval and consent to participate
This study is in approval with the Ethics Committee of the Affiliated Hospital of Qingdao University(approval number: QYFYWZLL26556). The patients have read and signed the informed consent form to participate.

Consent for publication
Not Applicable.

Competing interests
The authors declare no competing interests.

Received: 24 March 2024 Accepted: 12 March 2025
Published online: 19 March 2025

References

1. Rathmell WK, et al. Management of metastatic clear cell renal cell carcinoma: ASCO guideline. J Clin Oncol. 2022;40:2957–95.
2. Chen W, et al. Clinical significance, molecular characterization, and immune microenvironment analysis of coagulation-related genes in clear cell renal cell carcinoma. Cancer Innov. 2024;3:e105.
3. Xia C, et al. Cancer statistics in China and United States, 2022: profiles, trends, and determinants. Chin Med J. 2022;135:584–90.
4. Motzer RJ, et al. Kidney cancer, version 3.2022, NCCN clinical practice guidelines in oncology. J Natl Compr Cancer Ntwrk : JNCCN. 2022;20:71–90.
5. Bahadoram S, et al. Renal cell carcinoma: an overview of the epidemiology, diagnosis, and treatment. G Ital Nefrol. 2022;39:2022.
6. Hsieh JJ, et al. Renal cell carcinoma. Nat Rev Dis Primers. 2017;3:17009.
7. Schulz M, Diehl V, Trebicka J, Wygrecka M, Schaefer L. Biglycan: a regulator of hepatorenal inflammation and autophagy. Matrix Biol. 2021;100–101:150–61.
8. Appunni S, et al. Biglycan: an emerging small leucine-rich proteoglycan (SLRP) marker and its clinicopathological significance. Mol Cell Biochem. 2021;476:3935–50.
9. Little PJ, Osman N, O'Brien KD. Hyperelongated biglycan: the surreptitious initiator of atherosclerosis. Curr Opin Lipidol. 2008;19:448–54.

10. Shainer R, et al. Biglycan regulates bone development and regeneration. Front Physiol. 2023;14:1119368.
11. Scuruchi, M., Potì, F., Rodríguez-Carrio, J., Campo, G.M. & Mandraffino, G. Biglycan and atherosclerosis: lessons from high cardiovascular risk conditions. Biochim Biophys Acta. Mol Cell Biol Lipids. 2020;1865:158545.
12. Maishi N, Hida K. Tumor endothelial cells accelerate tumor metastasis. Cancer Sci. 2017;108:1921–6.
13. He ZX, et al. Prognostic and predictive value of BGN in colon cancer outcomes and response to immunotherapy. Front Oncol. 2021;11:761030.
14. He Z, et al. Identification of BGN and THBS2 as metastasis-specific biomarkers and poor survival key regulators in human colon cancer by integrated analysis. Clin Transl Med. 2022;12: e973.
15. Ma YS, et al. Proteogenomic characterization and comprehensive integrative genomic analysis of human colorectal cancer liver metastasis. Mol Cancer. 2018;17:139.
16. Liu B, Xu T, Xu X, Cui Y, Xing X. Biglycan promotes the chemotherapy resistance of colon cancer by activating NF-κB signal transduction. Mol Cell Biochem. 2018;449:285–94.
17. Navani S. Manual evaluation of tissue microarrays in a high-throughput research project: the contribution of Indian surgical pathology to the Human Protein Atlas (HPA) project. Proteomics. 2016;16:1266–70.
18. Sarbu M, Ica R, Sharon E, Clemmer DE, Zamfir AD. Glycomics by ion mobility tandem mass spectrometry of chondroitin sulfate disaccharide domain in biglycan. J Mass spectrom : JMS. 2023;58:e4908.
19. Wei Z, et al. Gene coexpression analysis offers important modules and pathway of human lung adenocarcinomas. J Cell Physiol. 2020;235:454–64.
20. Yang Y, Wang R, Feng L, Ma H, Fang J. LINC00460 promotes cell proliferation, migration, invasion, and epithelial-mesenchymal transition of head and neck squamous cell carcinoma via miR-320a/BGN axis. Onco Targets Ther. 2021;14:2279–91.
21. Hu L, et al. Biglycan enhances gastric cancer invasion by activating FAK signaling pathway. Oncotarget. 2014;5:1885–96.
22. Wu H, et al. BGN/FAP/STAT3 positive feedback loop mediated mutual interaction between tumor cells and mesothelial cells contributes to peritoneal metastasis of gastric cancer. Int J Biol Sci. 2023;19:465–83.
23. Appunni S, et al. Small leucine rich proteoglycans (decorin, biglycan and lumican) in cancer. Clin Chim Acta; Int J Clin Chem. 2019;491:1–7.
24. Wagner EF, Nebreda AR. Signal integration by JNK and p38 MAPK pathways in cancer development. Nat Rev Cancer. 2009;9:537–49.
25. Wu Y, et al. A network pharmacology approach and experimental validation to investigate the anticancer mechanism of Qi-Qin-Hu-Chang formula against colitis-associated colorectal cancer through induction of apoptosis via JNK/p38 MAPK signaling pathway. J Ethnopharmacol. 2024;319:117323.
26. Hammouda MB, Ford AE, Liu Y, Zhang JY. The JNK signaling pathway in inflammatory skin disorders and cancer. Cells. 2020;9:857.
27. Fan J, et al. Bruceine D induces lung cancer cell apoptosis and autophagy via the ROS/MAPK signaling pathway in vitro and in vivo. Cell Death Dis. 2020;11:126.
28. Zhou F, Wang L, Ge H, Zhang D, Wang W. H3K27 acetylation activated-CD109 evokes 5-fluorouracil resistance in gastric cancer via the JNK/MAPK signaling pathway. Environ Toxicol. 2023;38:2857–66.
29. Dvorak HF. Tumors: wounds that do not heal. Similarities between tumor stroma generation and wound healing. N Engl J Med. 1986;315:1650–1659.
30. Wang Q, Su C, Zhou C. Recent advances in immunotherapy for lung cancer. Cancer Innov. 2023;2:18–24.
31. Zeng-Brouwers J, et al. Evaluation of the in vitro and in vivo effects of Biglycan in innate immunity. Methods Mol Biol (Clifton, N.J.). 2023;2619:109–124.
32. Schaefer L, et al. The matrix component biglycan is proinflammatory and signals through Toll-like receptors 4 and 2 in macrophages. J Clin Investig. 2005;115:2223–33.
33. Zheng S, et al. Landscape of cancer-associated fibroblasts identifies the secreted biglycan as a protumor and immunosuppressive factor in triple-negative breast cancer. Oncoimmunology. 2022;11:2020984.
34. Huang HC, et al. BGN/TLR4/NF-B mediates epigenetic silencing of immunosuppressive Siglec ligands in colon cancer cells. Cells. 2020;9:397.
35. Monjaras-Avila CU, et al. The tumor immune microenvironment in clear cell renal cell carcinoma. Int J Mol Sci. 2023;24:7946.

Publisher's Note